Parametric and cascaded parametric interactions in a quasiperiodic optical superlattice

Y. Du, S. N. Zhu,[a] Y. Y. Zhu, P. Xu, C. Zhang, Y. B. Chen, Z. W. Liu, and N. B. Ming
National Laboratory of Solid State Microstructures, Nanjing University, Nanjing, 210093, People's Republic of China

X. R. Zhang, F. F. Zhang, and S. Y. Zhang
State Key Laboratory of Modern Acoustics and Institute of Acoustics, Nanjing University, Nanjing, 210093, People's Republic of China

(Received 12 October 2001; accepted for publication 2 July 2002)

Quasi-phase-matching optical parametric and cascaded parametric processes in a two-component quasiperiodic superlattice were studied in theory and experiment. This letter demonstrates how to obtain red at 666 nm and blue at 443 nm simultaneously from the superlattice using a 532 nm laser as a pump through these two processes mentioned above. The result confirms that some nonlinear frequency conversion processes occurring in a high-dimension $\chi^{(2)}$ nonlinear photonic crystal may be efficiently achieved in such a one-dimension quasiperiodic optical superlattice. © *2002 American Institute of Physics.* [DOI: 10.1063/1.1502007]

In the early days of nonlinear optics the generation of tunable light by optical parametric process was proposed by many pioneers.[1–3] Since then although the research on this field has made significant progress and the basic principles behind the optical parametric generation (OPG) have also been established for a long time, one has still devoted great efforts to develop new nonlinear materials. OPG have been mainly achieved in birefringence phase-matching (BPM) crystals. In the past ten years, quasi-phase-matching (QPM) was introduced into OPG as an alternative technique to BPM. QPM has advantages over BPM due to its higher gain, no "walkoff," and allowing an extensive range of the signal and idler frequency combinations to be accessed in a particular material by changing the grating period.

However, the studies of QPM-OPG have been restricted in a periodical optical superlattice, such as periodically poled $LiNbO_3$[4] and $KTiOPO_4$.[5] In our earlier work,[6] QPM scheme was extended from a periodic structure to a quasiperiodic one, which led to an efficient cascaded frequency upconversion-frequency tripling from fundamental wave. Frequency downconversion is a reverse process of upconversion. Energy and momentum conservation are still the fundamental conditions for this process. In this letter we use a general two-component quasiperiodic optical superlattice (QPOS) to achieve a QPM-OPG and a QPM cascaded parametric interaction simultaneously. Two predesigned reciprocals exist there, one for the generations of the signal and idler by QPM-OPG, and the other for the sum-frequency generation (SFG) of blue by frequency mixing of the idler and the pump. Our results show that this extension not only brings out new phenomena but also may lead to new applications of QPOS in nonlinear optics.

As known, a one-dimensional (1D) quasiperiodic lattice can be created by the projection of two-dimensional (2D) square lattice on a straight line.[7] The projection points on the straight line form two types of interval *a* and *b*. The arranged sequence of *a* and *b* depends on the projection angle θ. By analogy, a two-component QPOS is constructed from two building blocks *A* and *B* with the widths D_A and D_B, respectively. Both *A* and *B* contain a pair of 180° antiparallel domain. Assume that the widths of positive domains in all *A* and *B* blocks are the same, represented with l [Fig. 1(a)]. According to the projection theory, the reciprocals for this QPOS are $G_{m,n}=2\pi(m+n\tau)/D$, where $D=\tau D_A+D_B$ is the average structure parameter, *m* and *n* are two integers, and $\tau=\tan\theta$. Since θ is an adjustable parameter, it offers quasiperiodic structure additional design flexibility for QPM. In this case the QPM-OPG condition is

$$\Delta k_l=k_p-k_s-k_i-G_{m,n}=0, \tag{1}$$

where $k_l=2\pi n_l/\lambda_l$ $(l=p,s,i)$ are the wave vectors, the subscripts *p,s,i* represent the pump, signal, and idler, respectively.

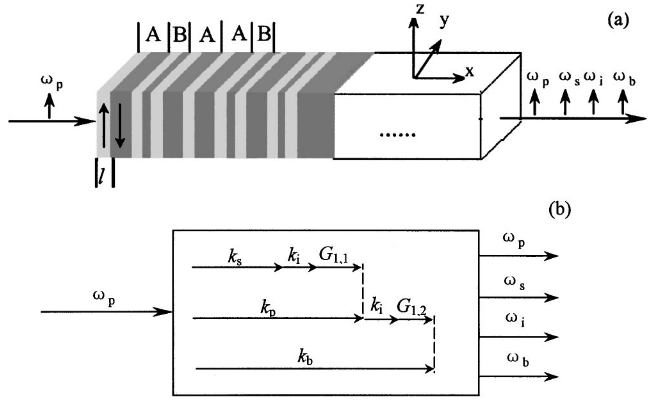

FIG. 1. QPOS made from a $LiTaO_3$ crystal. The arrows indicate the directions of spontaneous polarization: (a) schematic diagram shows a QPOS composed of two blocks A and B; (b) schematic diagram of the OPG and SFG processes, two QPM interactions are simultaneously realized which leads to a blue generation by frequency upconversion.

[a]Electronic mail: zhusn@netra.nju.edu.cn

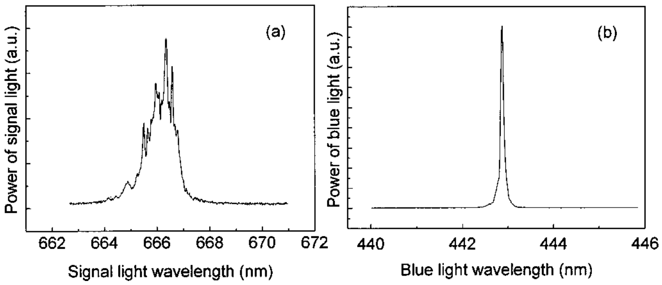

FIG. 2. Typical light spectrum observed at 38 °C: (a) signal light at 666 nm with the bandwidth 1.81 nm by OPG; (b) blue light at 443 nm with the bandwidth 0.08 nm by SFG.

In this work, for the first step, we aimed at the realization of red signal at 666 nm and of idler at 2644 nm by means of a 532 nm ps laser. According to $LiTaO_3$ dispersion feature and Eq. (1), the structure parameters of the QPOS were selected as: $D_A = 12.43\ \mu m$, $D_B = 8.63\ \mu m$, $l = 4.62\ \mu m$, and $\tau = 1.164$. The corresponding reciprocal is $G_{m,n} = G_{1,1}$. The phase-matching temperature is at 40 °C.

Although the selection of the above parameters is not unique for red signal generation, it does assure that the second QPM process, blue light by SFG can be realized in the structure:

$$\Delta k_2 = k_b - k_p - k_i - G_{m',n'} = 0, \tag{2}$$

where $G_{m',n'} = G_{1,2}$ is another predesigned reciprocal, k_b is the wave vector of the blue light. Two QPM processes, an OPG and a SFG, are simultaneously realized in the same superlattice in QPM scheme as shown in Fig. 1(b), and they are coupled to each other. Thus the pump at 532 nm is first transferred into the red at 666 nm, then the blue at 443 nm continuously in every part of such a QPOS.

The QPOS with the above structure parameters was fabricated using field poling technique at room temperature.[8] The quasiperiodic electrode, with 2.3 μm wide each stripe and along the y-axis of crystal, was defined on the $+z$ face by standard lithograph technique. The resulting sample is 0.5 mm in thickness, 2 cm in length. The sample was tested with the second-harmonic output of a ps-Nd:YAG laser (40 ps, 10 Hz). The pump beam was z polarized and propagated along the x axis of the sample. The beam was weakly focused and coupled into the polished end face of the sample. The focus of the focusing lens is 400 mm and the radius of the beam waist inside the sample was 0.1 mm around. The detector for spectrum measurement was a CCD spectrograph.

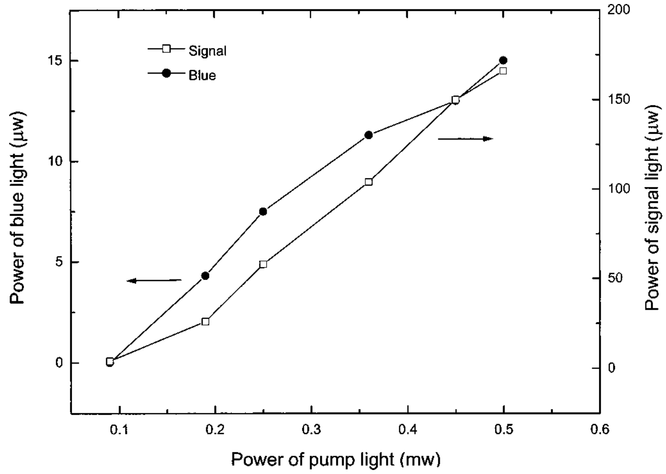

FIG. 3. Relationship between the power of the signal, blue light, and that of pump light.

The typical signal spectrum at 38 °C is shown in Fig. 2(a). The center wavelength of the red is 666 nm with the bandwidth of 1.81 nm. Wide bandwidth results from quantum fluctuation of OPG.[9] Limited by the operating range of our detector, we could not obtain the spectrum of the idler directly, but we can estimate its wavelength and bandwidth by signal spectrum measured. The blue spectrum with the peak at 443 nm and the bandwidth of 0.08 nm at the same temperature is shown in Fig. 2(b). Since the blue is the frequency mixing of idler and pump, the bandwidth of blue is mainly determined by that of pump due to the wide bandwidth of idler, and theoretically, it should be a little smaller than pump bandwidth. Experimentally, the measured bandwidths of pump and blue are about 0.1 and 0.08 nm, respectively, so the result agrees with the theoretical estimation.

In the limit of low gain, the single pass parametric gain is given as:[10]

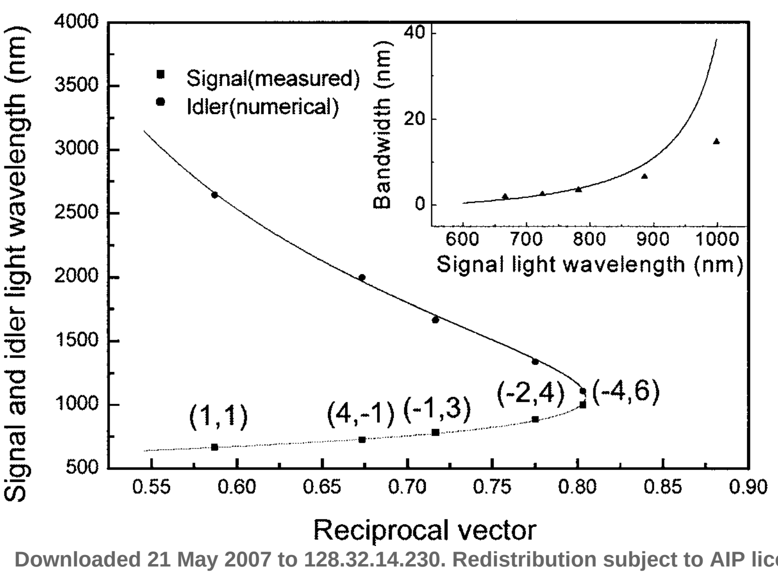

FIG. 4. Wavelengths of other signal light measured vs the corresponding reciprocal vectors $G_{m,n}$ labeled as (m, n). Inset, bandwidth of the measured signal wavelength marked with triangles. Solid lines are the result obtained by numerical calculation.

TABLE I. Experiment results of multiple parametric interactions in QPM-OPG in QPPLT.

Reciprocal Vectors $G_{m,n}$	Fourier component	Signal wavelength (nm)		Bandwidth (nm)	
		Calculated	Measured	Calculated	Measured
(1, 1)	0.477	665	666	1.23	1.81
(−1, 3)	0.047	729	725	2.28	2.50
(−2, 4)	0.027	774	782	3.81	3.5
(4, −1)	0.026	875	886	9.54	6.52
(−4, 6)	0.017	1012	999	38.60	14.71

$$G(L)=[E_s(L)/E_s(0)]^2-1 \sim \frac{2\omega_s\omega_i d^2(L)}{n_s n_i n_p \varepsilon_0 c^3} I_p L^2 \sin c^2(\Delta k L/2), \qquad (3)$$

where I_p is the pump intensity and L is the interaction length in the nonlinear crystal. It is obvious that the initial intensities for the signal and idler at the input plane of the material are equal to zero. It is necessary to consider the signal and idler generated at the beginning of the interaction as noise photons based on the quantum-mechanical model. In that way, the validity of Eq. (3) can be preserved. Figure 3 demonstrates the power of the signal is approximately proportional to that of pump, as expected by Eq. (3). The maximum conversion efficiency of the signal at the wavelength is up to 34.0% under the average pump power of 0.5 mW, meanwhile, that of blue is about 3.0%. The result obtained here can be compared with that from two periodic superlattices in series, either of them with a length $L/2$. The parametric gain at red in a QPOS is increased by a factor of $d_{1,1}^2 L^2/d_1^2(L/2)^2 \cong 2$ and $d_{1,1}^2 d_{1,2}^2 L^4/d_1^2 d_1^2 (L/2)^2 (L/2)^2 \cong 1.2$ at blue, respectively, here, $d_{1,1} \approx 0.74 d_1$ and $d_{1,2} \approx 0.39 d_1$, where d_1 is the greatest Fourier component of two-periodic superlattice. For more detailed discussions one can refer to Ref. 6.

Several other signal generations utilizing reciprocals other than $G_{1,1}$ were also detected in Fig. 4 showing the superlattice can provide a set of reciprocals for different QPM-OPG.[11] Table I lists these reciprocals indexed with two integers and their corresponding Fourier components that are directly proportional to their effective nonlinear coefficients. The measured wavelengths agree well with the calculated ones shown in the same figure. It certifies once again by the study that the reciprocal space structure in a QPOS is more abundant than that in a period structure.[11] Analogical phenomena were also found in a 2D $\chi^{(2)}$ photonic crystals,[12] showing a close relationship between the 1D quasiperiodic structure and 2D periodic structure. In addition, the bandwidths of signal measured above are also shown in Fig. 4. The corresponding theoretical values are given by[9]

$$B_\omega = \frac{2}{a}\left(\frac{2g_0}{L}\ln 2\right)^{1/2}, \quad a=\left[\left(\frac{dk_s}{d\omega_s}\right)_{\omega_s^0} - \left(\frac{dk_i}{d\omega_i}\right)_{\omega_i^0}\right], \qquad (4)$$

where B_ω and g_0 represent the bandwidth and threshold value of OPG, respectively, and ω represents the frequency of corresponding parametric light. Meanwhile we can see clearly the bandwidth monotonically increases with the increase of signal wavelength. The bandwidth of 999 nm is about ten times of that of 666 nm. When the signal light varies from lower wavelength to 1064 nm, which is the degeneracy, the bandwidth reaches its maximum. In theory, the signal and idler will not be distinguished in this point. Experimentally, we could not find the blue at other wavelength. This is easy to understand. Since the Fourier components of other reciprocals are much smaller than $G_{1,1}$ (Table I), the corresponding idlers at infrared are feebler, therefore, the blue lights generated by frequency mixing of pump and these idlers are too weak to be detected under our case.

Our result reveals that QPOS might find other applications in nonlinear optics and quantum optics. It may serve for a unique source applicable to the generation of correlated photon pairs, which is extremely useful for the study of quantum entanglement,[13] quantum interference,[14] quantum cryptography,[15] etc. due to its high gain. Another actual application of QPOS is served as nonlinear crystal for the three fundamental colors laser by QPM-OPG cascaded with a QPM-SFG as described in this letter. Moreover, it can be used to generate any color through a weighted combination of red, green, and blue in an optimized OPO system. In the same way, the superlattice crystal can be exploited in other tunable multicolor laser system.

This work is supported by a grant for the State Key Program for Basic Research of China, by the National Advanced Materials Committee of China, and by the National Natural Science Foundation of China (10021001). S. N. Zhu also thanks the support from the FANEDD(199921).

[1] R. A. Baumgartner and R. L. Byer, IEEE J. Quantum Electron. **15**, 432 (1979).
[2] J. A. Armstrong, N. Bloembergen, J. Ducuing, and P. S. Pershan, Phys. Rev. **127**, 1918 (1962).
[3] R. H. Kingston, Proc. IRE **50**, 472 (1962).
[4] L. E. Myers, G. D. Miller, R. C. Eckardt, M. M. Fejer, R. L. Byer, and W. R. Bosenberg, Opt. Lett. **20**, 52 (1995); J. Opt. Soc. Am. B **12**, 2102 (1995).
[5] H. Karlsson and F. Laurell, Appl. Phys. Lett. **71**, 3474 (1997).
[6] S. N. Zhu, Y. Y. Zhu, and N. B. Ming, Science **278**, 843 (1997).
[7] R. K. P. Zia and W. J. Dallas, J. Phys. A **18**, 341 (1985).
[8] K. P. Petrov, A. T. Ryan, T. L. Patterson, L. Huang, S. J. Field, and D. Bamford, Appl. Phys. B: Lasers Opt. **67**, 357 (1998).
[9] Y. R. Shen, *The Principles of Nonlinear Optics* (Wiley, New York, 1984), Vol. 9, p. 147.
[10] R. L. Byer, J. Nonlinear Opt. Phys. Mater. **6**, 549 (1997).
[11] S. N. Zhu, Y. Y. Zhu, Y. Q. Qin, H. F. Wang, C. Z. Ge, and N. B. Ming, Phys. Rev. Lett. **78**, 2752 (1997).
[12] V. Berger, Phys. Rev. Lett. **81**, 4136 (1998).
[13] K. Molmer, J. Mod. Opt. **44**, 1937 (1997).
[14] M. Casas, A. Plastino, J. Perez, and A. Rigo, Phys. A **269**, 476 (1999).
[15] Y. H. Shih and C. O. Alley, Phys. Rev. Lett. **61**, 2921 (1988).